UCHL1, a Deubiquitinating Enzyme, Regulates Lung Endothelial Cell Permeability *In Vitro* and *In Vivo*

Sumegha Mitra[1], Yulia Epshtein[2], Saad Sammani[3], Hector Quijada[3], Weiguo Chen[2], Mounica Bandela[2], Ankit A. Desai[4], Joe G.N.Garcia[3], Jeffrey R. Jacobson[2]

[1]Department of Biochemistry and Molecular Biology, Indiana University School of Medicine, Indianapolis, IN

[2]Department of Medicine, Division of Pulmonary, Critical Care, Sleep and Allergy, University of Illinois at Chicago, Chicago, IL

[3]Department of Medicine, Arizona Health Sciences Center, University of Arizona, Tucson, AZ USA

[4]Department of Medicine, Indiana University School of Medicine, Bloomington, IN

Running Head: UCHL1 regulates lung vascular permeability

Corresponding author:

Jeffrey R. Jacobson, M.D.
Professor of Medicine
Division of Pulmonary, Critical Care, Sleep and Allergy
University of Illinois, Chicago
College of Medicine Research Building, Room 3141
909 S. Wolcott Ave
Chicago, IL 60612
phone: 312-355-5892
e-mail: jrjacob@uic.edu

Keywords: UCHL1, endothelial cells, lung vascular permeability

Abstract

Increasing evidence suggests an important role for deubiquitinating enzymes (DUBs) in modulating a variety of biological functions and diseases. We previously identified the upregulation of the DUB, ubiquitin carboxyl terminal hydrolase 1 (UCHL1) in murine ventilator-induced lung injury (VILI). However, the role of UCHL1 in modulating vascular permeability, a cardinal feature of acute lung injury (ALI) in general, remains unclear. We investigated the role of UCHL1 in pulmonary endothelial cell (EC) barrier function *in vitro* and *in vivo* and examined effects of UCHL1 on VE-cadherin and claudin-5 regulation, important adherens and tight junctional components, respectively. Measurements of transendothelial electrical resistance (TER) confirmed decreased barrier enhancement induced by hepatocyte growth factor (HGF) and increased thrombin-induced permeability in both UCHL1-silenced EC and in EC pretreated with LDN-57444 (LDN), a pharmacologic UCHL1 inhibitor. Additionally, UCHL1 knockdown (siRNA) was associated with decreased expression of VE-cadherin and claudin-5 while silencing of the transcription factor, FoxO1 restored claudin-5 levels. Finally, UCHL1 inhibition *in vivo* via LDN was associated with increased VILI in a murine model. These findings support a prominent functional role of UCHL1 in regulating lung vascular permeability via alterations in adherens and tight junctions and implicate UCHL1 as an important mediator of ALI.

Introduction

Acute lung injury (ALI) is a debilitating condition encountered in critically ill patients and represents a significant cause of ICU-related morbidity and mortality (17). Aberrant vascular permeability and inflammation that impairs alveolar gaseous exchange are critical elements of ALI. Mechanical ventilation, frequently utilized in critically ill patients, can precipitate and aggravate ALI due to excessive mechanical stress, a condition known as ventilation-induced lung injury (VILI) (11). Despite improved recognition of this syndrome, effective therapies remain lacking and ALI is estimated to account for approximately 75,000 deaths and millions of hospital days per year in the United States (26). Moreover, ALI survivors have been found to have impaired lung function, neuropsychological deficits and decreased quality of life long term (9, 19). Thus, novel therapeutic targets and strategies aimed at improving pulmonary endothelial barrier function may prove beneficial in mitigating the effects of increased vascular leak associated with ALI and may ultimately lead to improved clinical outcomes.

Utilizing global gene expression profiling we previously identified growth arrest DNA damage inducible 45 alpha (GADD45a) as a significantly upregulated gene in pre-clinical models of VILI (13). We subsequently reported increased VILI susceptibility of GADD45a$^{-/-}$ mice (20). Further *in silico* analysis identified reduced levels of ubiquitin carboxyl-terminal hydrolase 1 (UCHL1), a deubiquitinating enzyme (DUB), in GADD45a$^{-/-}$ animals. Decreased UCHL1 levels were found to be due to the hypermethylation of the UCHL1 promoter which, in turn, is associated with increased Akt K48 ubiquitination

and subsequent proteasomal degradation. Additionally, treatment of GADD45a$^{-/-}$ mice with 5-Aza-deoxycytidine (5-AZA-DC), a DNA methyl transferase inhibitor, both significantly increased UCHL1 levels and attenuated VILI susceptibility.

Functionally, UCHL1 removes or edits poly- or mono-ubiquitin chains from ubiquitinated proteins that may regulate a range of cellular processes including cell cycle, DNA repair, cell-cell communication and apoptosis (7, 23). While UCHL1 has been implicated in a variety of diseases including neurodegenerative disorders, lung cancer and colon cancer (15, 29), its role in ALI had not previously been reported. We investigated the role of UCHL1 in regulation of endothelial cell (EC) permeability. We studied the effects of UCHL1 silencing and inhibition on human pulmonary artery EC permeability by measuring transendothelial resistance. We also explored the role of UCHL1 in regulating adherens and tight junctional proteins, VE-cadherin and claudin-5, respectively. Finally, we investigated the potential effects of LDN-57444 (LDN) a pharmacologic UCHL1 inhibitor in murine VILI.

Materials and Methods

Antibodies and reagents. Antibodies and reagents were purchased commercially consistent with our prior reports [7,15]. Antibodies against UCHL1 (Cell Signaling, Danvers, MA), VE-cadherin (Santa Cruz Biotechnology, Santa Cruz, CA), Y658 VE-cadherin (Biosource, Grand Island, NY), β-catenin (Santa Cruz Biotechnology, Santa Cruz, CA), FoxO1 (Cell Signaling, Danvers, MA), phospho-FoxO 1 (Cell Signaling, Danvers, MA), β-actin (Sigma, St. Louis, MO), claudin-5 (Cell Signaling), horseradish peroxidase-conjugated anti-mouse and anti-rabbit secondary antibodies (Cell Signaling) were purchased from the indicated vendors. A smart pool of silencing RNA (siRNA) specific for UCHL1, FoxO1 and non-specific siRNA were purchased from GE Dharmacon (Lafayette, CO). Other reagents used include the proteasome inhibitor MG132 (Calbiochem, San Diego, CA), LDN-57444 (LDN, Calbiochem, San Diego, CA), hepatocyte growth factor (HGF) (Peprotech, Rocky Hill, NJ) and thrombin (Sigma, St. Louis, MO).

Endothelial cell culture. Human pulmonary artery endothelial cells (EC) were cultured in essential growth medium (EGM-2) containing 10% fetal bovine serum (Clonetics, Walkersville, MD). Cells were placed in incubator at 37°C, 5% CO_2 and 95% humidity to achieve contact-inhibited monolayers. Select experiments utilized human lung microvascular endothelial cells (HLMVEC, Lonza, Hayward, CA).

Endothelial cell (EC) siRNA transfection and treatment with a UCHL1 inhibitor. EC were transfected with siRNA (100 nM, GE Dharmacon, Lafayette, CO) specific for UCHL1, FoxO1 or non-specific scrambled sequence using transfection reagent siPORT *Amine* (Ambion, Austin, TX) in serum-free conditions according to the manufacturer's protocol. The medium was changed to EGM-2 containing 2% fetal bovine serum after 24 hours of transfection and protein silencing was checked after 72 hours of transfection. Silenced cells were plated on the ECIS polycarbonate wells and transwell cell culture insert after 48 h of transfection and assays were performed after 24 h. UCHL1 inhibitor, LDN, was dissolved in 60% DMSO and EC were treated (5 μM) for 1.5 h. 60% DMSO was used as vehicle control.

Transendothelial electrical resistance (TER) measurement. EC were plated into polycarbonate wells containing evaporated gold microelectrodes to measure TER that evaluates real-time changes in cell morphology, attachment and locomotion using an electric cell-substrate impedence system (ECIS) (Applied Biophysics, Troy, NY) as previously described (12). Cells were grown to confluence in EBM-2 containing 2% serum. TER values from each microelectrode were pooled at discrete time-points and plotted versus time as the mean ± SEM. EC monolayers were treated with hepatocyte growth factor (HGF, 25 ng/ml) or thrombin (1 U/ml), agonists that enhance or disrupt barrier integrity, respectively.

Immunoblotting and immunoprecipitation. As we have previously described [7], total proteins were extracted using NP-40 lysis buffer (50 mM TrisHCl pH 7.4, 150 mM NaCl,

1% NP-40, and 5 mM ethylenediaminetetraacetic acid) supplemented with 40 mM sodium fluoride, 0.1 M Sodium Orthovanadate, 0.2 mM phenylmethylsulfonyl fluoride, 10 mM N' ethyl malamide, and protease and phosphatase inhibitor cocktail (Calbiochem, San Diego, CA). Lung homogenates and cell lysates were briefly sonicated and were subjected to cycles of thawing and freezing on dry ice. The protein concentrations were measured using bicinchoninic acid protein assay kit (Pierce, Rockford, IL). Western blotting was performed using standard protocols and bands densities were determined using ImageJ (National Institutes of Health, http://imagej.nih.gov/ij/). For immunoprecipitation, proteins were extracted in RIPA buffer (50 mM Tris-HCL, pH 7.4, 150 mM NaCl, 1% NP-40, 0.5% Sodium deoxycholate, 0.1% SDS with protease and phosphatase inhibitor cocktails) and immunoprecipitation was performed, after pre-clearing with protein A/G Sepharose beads, by incubating protein extracts with primary antibodies (2 mg) overnight at 4°C. Immunocomplexes were collected by incubating with protein A/G Sepharose beads for 1 hour at 4°C and were resolved by polyacrylamide gel electrophoresis followed by Western blotting.

Immunofluorescence. Cells were fixed with 4% paraformaldehyde (pH 7.0) for 20 min, permeabilized with 0.2% triton X-100, and blocked with 5% bovine serum albumin for 1 h followed by overnight incubation at 4°C with primary antibodies as we have previously described [7,15]. Cells were incubated with goat anti-rabbit Alexa Fluor 635 and goat anti-mouse Alexa Fluor 488 secondary antibodies for 1 h. Nuclei were stained with Hoechst 33342 and coverslips were mounted on slides using mounting solution prolong

gold. Cells were then imaged using a Carl Zeiss LSM 510 laser scanning confocal microscope (Göttingen, Germany).

Pre-clinical VILI model. Male, 8 to 12 week-old C57BL/6 mice (Jackson Laboratory, Bar Harbor, ME) were anesthetized with an intraperitoneal (IP) mix of ketamine (150 mg/kg) and xylazine (15 mg/kg) prior to intubation with a 20 gauge angiocatheter which was then attached to a small animal mechanical ventilator (Harvard Apparatus, Holliston, MA) with V_T = 30 ml/kg, 65 breaths per minute, and positive end-expiratory pressure of 0 cm H_2O for 4 h as previously described (18, 20). Mice were treated with LDN (5 mg/kg, IP) or vehicle 24 h and 1 h before VILI-challenge. Notably, this dosing of LDN is consistent with dosing used by other investigators *in vivo* (4, 25). Bronchoalveolar lavage (BAL) fluid was collected and assessed for total protein as well as total and differential cell counts as previously described (18). All experiments and animal care procedures were approved by the University of Illinois at Chicago Animal Care and Use Committee and were performed in accordance with *Guide for the Care and Use of Laboratory Animals, Eighth Edition* published by the Institute for Laboratory Animal Research.

Murine lung histology. As we have previously reported (5), lung tissue samples were fixed in formalin, embedded in paraffin, cut into 10 μm sections, and stained with hematoxylin and eosin (H&E). Histology slides were scanned and evaluated with ImageScope (Aperio, Vista, CA). H&E stained lung sections (n = 6-10 per condition) were visualized and representative images are provided.

Statistics. Unless otherwise stated, Student's t-test was used to compare the means of data from two experimental groups while significant differences ($p < 0.05$) amongst multiple group comparisons were confirmed by one-way ANOVA followed by Tukey's range test consistent with our prior reports [7,15]. Results are expressed as means $\pm$ SE.

Results

UCHL1 knockdown and EC barrier function. To determine the role of UCHL1 in regulating EC permeability, human pulmonary artery EC were transfected with siRNA specific for UCHL1 or a control siRNA and then grown to confluence overlying gold-plated microelectrodes. Cells were then treated with either HGF (25 ng/ml) or thrombin (1 U/ml) to effect barrier enhancement or disruption, respectively, and normalized TER was measured (**Figure 1**). A significant increase in TER was observed in control EC after HGF. However, peak HGF response (at 45 min) was significantly attenuated in UCHL1-silenced cells compared to controls. Similarly, TER nadir and time to recovery after treatment with thrombin (1 U/ml), a barrier-disrupting agent, was significantly increased in UCHL1-silenced cells compared to unsilenced cells. Moreover, UCHL1 silencing was associated with a significant reduction in basal TER measurements compared to control cells. Notably, these experiments were repeated utilizing human lung microvascular endothelial cells with the same experimental conditions and confirmed a similar effect of UCHL1 knockdown, both qualitatively and quantitatively, on microvascular EC barrier regulation (**Figure 1D**).

UCHL1 inhibition with LDN and EC barrier function. Next, experiments were repeated using LDN-57444 (LDN), a pharmacologic inhibitor of UCHL1 activity (**Figure 2**). TER measurements of EC treated with LDN (5 μM, 1.5 h) prior to either HGF (25 ng/ml) or thrombin (1 U/ml) demonstrated a significant attenuation of HGF-induced barrier enhancement and augmentation of thrombin-induced disruption. Baseline TER

measurements were unchanged in LDN-treated cells compared to controls. Together, these results highlight the negative regulatory effects of UCHL1 silencing and inhibition on EC barrier function.

Redistribution of VE-cadherin and β-catenin in UCHL1-silenced EC. EC maintain cell-cell contact and monolayer integrity via both adherens junction (AJ) and tight junctions (TJ). We next studied the role of UCHL1 in the spatial localization of VE-cadherin and β-catenin, two major AJ proteins, using confocal microscopy. Immunofluorescence images of control EC revealed prominent membrane co-localization of VE-cadherin and β-catenin (**Figure 3A**). However, UCHL1 silencing was notable for reduced levels of VE-cadherin and β-catenin at the membrane with a relative increase in the cytoplasmic distribution of both. In addition, Western blotting confirmed significantly reduced total VE-cadherin levels in UCHL1-silenced EC although no significant change was observed in β-catenin levels (**Figure 3B**).

Role of UCHL1 in VE-cadherin phosphorylation and ubiquitination. Junctional weakness and VE-cadherin internalization are associated with tyrosine phosphorylation of VE cadherin (1). In response to UCHL1 silencing, we next studied VE-cadherin phosphorylation at tyrosine 658 (Y658) and investigated the mechanism underlying the associated decreased VE-cadherin expression levels. We observed a significant increase in Y658 phosphorylation of VE-cadherin in UCHL1-silenced cells with a concomitant decrease in total VE cadherin (**Figure 4**). Subsequently, we treated UCHL1-silenced EC with chloroquine (20 μM, 2 h) or MG132 (10 μM, 2 h), lysosome

and proteasome inhibitors, respectively, as VE-cadherin is known to be degraded both the endosomal/lysosomal pathway (32) and the ubiquitin-proteasomal pathway (22). While no changes in VE-cadherin levels were observed with chloroquine treatment, the decreased levels of VE-cadherin in UCHL1-silenced cells were significantly rescued by MG132. Further, increased ubiquitination of VE-cadherin was evident upon the immunoprecipitation of VE-cadherin in UCHL1-silenced EC (**Figure 4C**). Collectively, these results implicate UCHL1 as important for the maintenance and regulation of AJ via effects on VE-cadherin including its cellular localization, phosphorylation, as well as its ubiquitination and proteasomal degradation. Although we did not investigate the mechanisms underlying increased VE-cadherin phosphorylation despite decreased total VE-cadherin in these experiments, we speculate that increased proteasomal degradation of VE-cadherin promotes its internalization from the membrane, an event known to be associated with increased phosphorylation [12].

Tight junctional protein expression and regulation in UCHL1-silenced EC. Claudins are the major transmembrane proteins of TJ that regulate paracellular permeability, cell polarity, and signal transduction (2). VE-cadherin spatial distribution is known to mediate claudin-5 expression regulated by the transcription factor, FoxO1 (5, 27). Accordingly, we next assessed the role of UCHL1 in the regulation claudin-5 expression. Western blotting revealed significantly reduced claudin-5 protein levels in UCHL1-silenced EC compared to unsilenced controls (**Figure 5A**). Further, fluorescent images confirmed a significant reduction of claudin-5 expression at the cell periphery in UCHL1-silenced cells compared to unsilenced cells (**Figure 5B**). Thus, VE-cadherin

cytoplasmic distribution in UCHL1-silenced EC correlates with reduced claudin-5 expression consistent with our prior report (5).

VE-cadherin internalization and degradation is known to promote accumulation of β-catenin and unphosphorylated FoxO1 in the nucleus, which transcriptionally inhibit claudin-5 expression (27). To study the regulation of claudin-5 by FoxO1 in UCHL1-silenced EC, we silenced FoxO1 and UCHL1, separately and in combination, and assessed claudin-5 expression levels by Western blotting. Notably, FoxO1-silencing abrogated claudin-5 downregulation in UCHL1-silenced EC (**Figure 5C**).

Role of UCHL1 in the elaboration of murine VILI. To study the role of UCHL1 in the elaboration of vascular permeability and inflammation associated with VILI *in vivo* wildtype C57Bl/6 mice were treated with LDN-57444 (5 mg/kg, IP) or vehicle 24 h and again 1 h before VILI-challenge (V_T 30 ml/kg, 4 h). A small but significant increase in BAL fluid protein levels was observed in control (spontaneously breathing) mice treated with LDN compared to untreated controls while there was no difference in BAL total cell counts or neutrophils. Most notably, amongst VILI-challenged mice LDN treatment was associated with significantly increased BAL fluid total protein levels, total cell counts and polymorphonuclear neutrophils (PMN) compared to vehicle-treated (**Figure 6**). In addition, evaluation of lung histology of VILI-challenged mice also confirmed significantly increased alveolar and interstitial inflammatory cells associated with LDN treatment compared to vehicle-treated controls (**Figure 7**). These data support the idea that inhibition of UCHL1 *in vivo* increases VILI susceptibility as characterized by

augmented lung vascular permeability and inflammation, an observation consistent with our *in vitro* findings.

Discussion

Research aimed at characterizing the molecular mechanisms that regulate pulmonary endothelial barrier function offers the promise of identifying novel therapeutic targets to treat the dire clinical effects of increased vascular leak associated with ALI. We previously identified UCHL1 as significantly upregulated in response to excessive mechanical stress in a pre-clinical VILI model (20). Moreover, increased VILI susceptibility was associated with reduced UCHL1 expression as we reported in GADD45a$^{-/-}$ mice. These animals express decreased UCHL1 due to promoter hypermethylation while GADD45a$^{-/-}$ mice treated with a DNA methylase inhibitor were found to have increased UCHL1 levels and reduced VILI susceptibility (20). Our results now strongly support an important role for UCHL1 in EC barrier regulation and suggest UCHL1 may represent a novel therapeutic target in ALI.

UCHL1 is a deubiquitinating enzyme that negatively regulates protein ubiquitination and thus has effects on ubiquitin-dependent signaling, protein stability and ubiquitin homeostasis (7). Expression of UCHL1 is most prevalent in the brain, comprising as much as 5-10% of neuronal proteins (8), and it has been implicated as a pathogenic molecule in neurodegenerative disorders including both Alzheimer's and Parkinson's diseases as well as Lewy body disease (6, 24, 31). While low levels of UCHL1 expression are found in other tissues, increased expression has been reported in a variety of cancers including pancreas, colorectal and breast cancer (10, 21, 34).

Conversely, decreased UCHL1 expression due to hypermethylaton of the promoter has been linked to ovarian, nasopharyngeal and gastric cancers, among others (8, 16, 33). Interestingly, increased UCHL1 expression has also been linked to improved outcomes in patients with neuroblastoma (3). While there is evidence that vascular remodeling may be attenuated by UCHL1 through inhibition of NF-κB (28), the role of UCHL1 in vascular biology in general has been poorly characterized.

We found that UCHL1 is protective in models of increased lung vascular permeability as both knockdown of UCHL1 (siRNA) and its pharmacologic inhibition (LDN) were associated with increased vascular leak both *in vitro* and *in vivo*. Our findings were also associated with increased ubiquitination and decreased expression levels of VE-cadherin, an adherens junction protein that regulates vascular permeability via Y658 phosphorylation (30). Further, UCHL1 knockdown was associated with decreased expression of claudin-5, an effect reversed by silencing of the transcriptional repressor, FoxO1 (**Figure 8**). These data are consistent with the known regulation of claudin-5 expression by VE-cadherin via the inhibition of the nuclear accumulation of FoxO1 (27).

One limitation of our study is the use of siRNA and pharmacologic inhibitors, both of which have potential non-specific or off-target effects. However, the comparable results we observed employing these separate strategies support the likelihood that these results are in fact due to decreased UCHL1 activity. Another potential limitation is the fact that it could be argued that our *in vivo* results do not confirm effects of LDN on lung

vascular permeability directly. However, evidence of increased levels of both protein and inflammatory cells in the BAL from VILI-challenged animals that received LDN is undoubtedly strong evidence of increased lung vascular permeability due to LDN treatment since these effects simply could not occur otherwise.

Separately, while our data supports the idea that UCHL1 regulates VE-cadherin and claudin-5, another limitation of the current study is that these effects were also not confirmed in our *in vivo* experiments. However, we previously found significant increases in expression levels of both VE-cadherin and claudin-5 in lung homogenates from GADD45a$^{-/-}$ mice associated with overexpression of UCH1. Moreover, the importance of VE-cadherin, claudin-5 and FoxO1 as mediators of lung vascular permeability are supported by our prior work related to simvastatin, an HMG-coA reductase inhibitor that continues to have tantalizing yet unproven potential as a treatment for ALI (3, 5). Notably, mice with a targeted deletion of FoxO1 in the endothelium were found to have decreased lung vascular leak and mortality in a pre-clinical sepsis model [Regmi et al, preprint article]. In addition, numerous investigators have reported promising findings related to the therapeutic potential of a variety of agonists in lung injury models that also effect these molecules and their associated signaling. One recent example is nicorandil, a nitrate used to treat angina and ATP-sensitive K^+ channel agonist, that was reported to be both protective in a pre-clinical ALI model and to increase VE-cadherin expression in lung EC (14). Nonetheless, the

realization of a safe and effective pharmacologic treatment for ALI remains an unmet goal.

We have for the first time identified effects on the elaboration of lung injury associated with the targeted inhibition of UCHL1, a DUB that has previously garnered much interest in the cancer literature but has otherwise not previously been studied in this context. While these findings are novel, we recognize that the immediate translational applications may be limited. Nonetheless, it is clear that research focused on strategies aimed at effecting increased UCHL1, either its expression or activity, are now needed and investigations in this area may ultimately

Acknowledgements

Research reported in this publication was supported by the National Heart, Lung, and Blood Institute of the National Institutes of Health under award number R01 HL147942 (JJ, YE, WC).

References

1. **Allingham MJ, van Buul JD, and Burridge K**. ICAM-1-mediated, Src- and Pyk2-dependent vascular endothelial cadherin tyrosine phosphorylation is required for leukocyte transendothelial migration. *J Immunol* 179: 4053-4064, 2007.

2. **Bazzoni G**. Endothelial tight junctions: permeable barriers of the vessel wall. *Thromb Haemost* 95: 36-42, 2006.

3. **Calfee CS, Delucchi KL, Sinha P, Matthay MA, Hackett J, Shankar-Hari M, McDowell C, Laffey JG, O'Kane CM, McAuley DF, and Irish Critical Care Trials G**. Acute respiratory distress syndrome subphenotypes and differential response to simvastatin: secondary analysis of a randomised controlled trial. *Lancet Respir Med* 6: 691-698, 2018.

4. **Cartier AE, Ubhi K, Spencer B, Vazquez-Roque RA, Kosberg KA, Fourgeaud L, Kanayson P, Patrick C, Rockenstein E, Patrick GN, and Masliah E**. Differential effects of UCHL1 modulation on alpha-synuclein in PD-like models of alpha-synucleinopathy. *PLoS One* 7: e34713, 2012.

5. **Chen W, Sharma R, Rizzo AN, Siegler JH, Garcia JG, and Jacobson JR**. Role of claudin-5 in the attenuation of murine acute lung injury by simvastatin. *Am J Respir Cell Mol Biol* 50: 328-336, 2014.

6. **Choi J, Levey AI, Weintraub ST, Rees HD, Gearing M, Chin LS, and Li L**. Oxidative modifications and down-regulation of ubiquitin carboxyl-terminal hydrolase L1 associated with idiopathic Parkinson's and Alzheimer's diseases. *J Biol Chem* 279: 13256-13264, 2004.

7. **Clague MJ, Coulson JM, and Urbe S**. Cellular functions of the DUBs. *J Cell Sci* 125: 277-286, 2012.

8. **Day IN, and Thompson RJ**. UCHL1 (PGP 9.5): neuronal biomarker and ubiquitin system protein. *Prog Neurobiol* 90: 327-362, 2010.

9. **Dowdy DW, Eid MP, Dennison CR, Mendez-Tellez PA, Herridge MS, Guallar E, Pronovost PJ, and Needham DM**. Quality of life after acute respiratory distress syndrome: a meta-analysis. *Intensive Care Med* 32: 1115-1124, 2006.

10. **Finnerty BM, Moore MD, Verma A, Aronova A, Huang S, Edwards DP, Chen Z, Seandel M, Scognamiglio T, Du YN, Elemento O, Zarnegar R, Min IM, and Fahey TJ**. UCHL1 loss alters the cell-cycle in metastatic pancreatic neuroendocrine tumors. *Endocr Relat Cancer* 26: 411-423, 2019.

11. **Gajic O, Dara SI, Mendez JL, Adesanya AO, Festic E, Caples SM, Rana R, St Sauver JL, Lymp JF, Afessa B, and Hubmayr RD**. Ventilator-associated lung injury in patients without acute lung injury at the onset of mechanical ventilation. *Crit Care Med* 32: 1817-1824, 2004.

12. **Garcia JG, Liu F, Verin AD, Birukova A, Dechert MA, Gerthoffer WT, Bamberg JR, and English D**. Sphingosine 1-phosphate promotes endothelial cell barrier integrity by Edg-dependent cytoskeletal rearrangement. *J Clin Invest* 108: 689-701, 2001.

13. **Grigoryev DN, Ma SF, Irizarry RA, Ye SQ, Quackenbush J, and Garcia JG**. Orthologous gene-expression profiling in multi-species models: search for candidate genes. *Genome Biol* 5: R34, 2004.

14. **He M, Shi W, Yu M, Li X, Xu J, Zhu J, Jin L, Xie W, and Kong H**. Nicorandil Attenuates LPS-Induced Acute Lung Injury by Pulmonary Endothelial Cell Protection via NF-kappaB and MAPK Pathways. *Oxid Med Cell Longev* 2019: 4957646, 2019.

15. **Jara JH, Frank DD, and Ozdinler PH**. Could dysregulation of UPS be a common underlying mechanism for cancer and neurodegeneration? Lessons from UCHL1. *Cell Biochem Biophys* 67: 45-53, 2013.

16. **Jin C, Yu W, Lou X, Zhou F, Han X, Zhao N, and Lin B**. UCHL1 Is a Putative Tumor Suppressor in Ovarian Cancer Cells and Contributes to Cisplatin Resistance. *J Cancer* 4: 662-670, 2013.

17. **Matthay MA, Zemans RL, Zimmerman GA, Arabi YM, Beitler JR, Mercat A, Herridge M, Randolph AG, and Calfee CS**. Acute respiratory distress syndrome. *Nat Rev Dis Primers* 5: 18, 2019.

18. **Meyer NJ, Huang Y, Singleton PA, Sammani S, Moitra J, Evenoski CL, Husain AN, Mitra S, Moreno-Vinasco L, Jacobson JR, Lussier YA, and Garcia JG**. GADD45a is a novel candidate gene in inflammatory lung injury via influences on Akt signaling. *FASEB J* 23: 1325-1337, 2009.

19. **Mikkelsen ME, Christie JD, Lanken PN, Biester RC, Thompson BT, Bellamy SL, Localio AR, Demissie E, Hopkins RO, and Angus DC**. The adult respiratory distress syndrome cognitive outcomes study: long-term neuropsychological function in survivors of acute lung injury. *Am J Respir Crit Care Med* 185: 1307-1315, 2012.

20. **Mitra S, Sammani S, Wang T, Boone DL, Meyer NJ, Dudek SM, Moreno-Vinasco L, Garcia JG, and Jacobson JR**. Role of growth arrest and DNA damage-inducible alpha in Akt phosphorylation and ubiquitination after mechanical stress-induced vascular injury. *Am J Respir Crit Care Med* 184: 1030-1040, 2011.

21. **Miyoshi Y, Nakayama S, Torikoshi Y, Tanaka S, Ishihara H, Taguchi T, Tamaki Y, and Noguchi S**. High expression of ubiquitin carboxy-terminal hydrolase-L1 and -L3 mRNA predicts early recurrence in patients with invasive breast cancer. *Cancer Sci* 97: 523-529, 2006.

22. **Orsenigo F, Giampietro C, Ferrari A, Corada M, Galaup A, Sigismund S, Ristagno G, Maddaluno L, Koh GY, Franco D, Kurtcuoglu V, Poulikakos D, Baluk P, McDonald D, Grazia Lampugnani M, and Dejana E**. Phosphorylation of VE-cadherin is modulated by haemodynamic forces and contributes to the regulation of vascular permeability in vivo. *Nat Commun* 3: 1208, 2012.

23. **Pfoh R, Lacdao IK, and Saridakis V**. Deubiquitinases and the new therapeutic opportunities offered to cancer. *Endocr Relat Cancer* 22: T35-54, 2015.

24. **Ragland M, Hutter C, Zabetian C, and Edwards K**. Association between the ubiquitin carboxyl-terminal esterase L1 gene (UCHL1) S18Y variant and Parkinson's Disease: a HuGE review and meta-analysis. *Am J Epidemiol* 170: 1344-1357, 2009.

25. **Reynolds JP, Jimenez-Mateos EM, Cao L, Bian F, Alves M, Miller-Delaney SF, Zhou A, and Henshall DC**. Proteomic Analysis After Status Epilepticus Identifies UCHL1 as Protective Against Hippocampal Injury. *Neurochem Res* 42: 2033-2054, 2017.

26. **Rubenfeld GD, Caldwell E, Peabody E, Weaver J, Martin DP, Neff M, Stern EJ, and Hudson LD**. Incidence and outcomes of acute lung injury. *N Engl J Med* 353: 1685-1693, 2005.

27. **Taddei A, Giampietro C, Conti A, Orsenigo F, Breviario F, Pirazzoli V, Potente M, Daly C, Dimmeler S, and Dejana E**. Endothelial adherens junctions control tight junctions by VE-cadherin-mediated upregulation of claudin-5. *Nat Cell Biol* 10: 923-934, 2008.

28. **Takami Y, Nakagami H, Morishita R, Katsuya T, Cui TX, Ichikawa T, Saito Y, Hayashi H, Kikuchi Y, Nishikawa T, Baba Y, Yasuda O, Rakugi H, Ogihara T, and Kaneda Y**. Ubiquitin carboxyl-terminal hydrolase L1, a novel deubiquitinating enzyme in the vasculature, attenuates NF-kappaB activation. *Arterioscler Thromb Vasc Biol* 27: 2184-2190, 2007.

29. **Tokumaru Y, Yamashita K, Kim MS, Park HL, Osada M, Mori M, and Sidransky D**. The role of PGP9.5 as a tumor suppressor gene in human cancer. *Int J Cancer* 123: 753-759, 2008.

30. **Wessel F, Winderlich M, Holm M, Frye M, Rivera-Galdos R, Vockel M, Linnepe R, Ipe U, Stadtmann A, Zarbock A, Nottebaum AF, and Vestweber D**. Leukocyte extravasation and vascular permeability are each controlled in vivo by different tyrosine residues of VE-cadherin. *Nat Immunol* 15: 223-230, 2014.

31. **Xia Q, Liao L, Cheng D, Duong DM, Gearing M, Lah JJ, Levey AI, and Peng J**. Proteomic identification of novel proteins associated with Lewy bodies. *Front Biosci* 13: 3850-3856, 2008.

32. **Xiao K, Allison DF, Kottke MD, Summers S, Sorescu GP, Faundez V, and Kowalczyk AP**. Mechanisms of VE-cadherin processing and degradation in microvascular endothelial cells. *J Biol Chem* 278: 19199-19208, 2003.

33. **Yamashita K, Park HL, Kim MS, Osada M, Tokumaru Y, Inoue H, Mori M, and Sidransky D**. PGP9.5 methylation in diffuse-type gastric cancer. *Cancer Res* 66: 3921-3927, 2006.

34. **Zhong J, Zhao M, Ma Y, Luo Q, Liu J, Wang J, Yuan X, Sang J, and Huang C**. UCHL1 acts as a colorectal cancer oncogene via activation of the beta-catenin/TCF pathway through its deubiquitinating activity. *Int J Mol Med* 30: 430-436, 2012.

Figure Legends

Figure 1. UCHL1 knockdown negatively impacts EC barrier regulation. (A) EC were transfected with siRNA specific for UCHL1 (siUCHL1, 100 nM, 3 d) or non-specific siRNA and were then subjected to Western blotting for UCHL1 to confirm silencing (representative blot shown). (B) Subsequently, EC transfected with either siUCHL1 or nsRNA were plated on polycarbonate wells containing evaporated gold microelectrodes followed by treatment with HGF (25 ng/ml), a barrier-enhancing agonist, or vehicle and transendothelial resistance (TER) was measured over time. At peak effect, HGF-induced barrier enhancement was significantly attenuated in UCHL1-silenced cells compared to controls (bar graph, *$p < 0.05$, n= 3). (C) In similar experiments, cells were treated with thrombin (1 U/ml), a barrier-disruptive agonist, or vehicle and TER was measured. At the nadir of TER changes, thrombin-induced barrier disruption was significantly increased (i.e. more disruption) in UCHL-1 silenced cells (bar graph, *$p < 0.05$, $n = 3$). (D) Experiments were repeated using human lung microvascular EC (HLMVEC) which confirmed similar effects on barrier regulation (representative tracings shown).

Figure 2. UCHL1 inhibition negatively impacts endothelial cell barrier regulation. (A) EC were plated on polycarbonate wells containing evaporated gold microelectrodes followed by treatment with the UCHL1 inhibitor, LDN 57444 (LDN, 5 μM) 1.5 h prior to HGF (25 ng/ml) and TER was measured over time. At peak effect, HGF-induced barrier

enhancement was significantly attenuated in LDN-treated cells compared to untreated controls (bar graph, *p < 0.05, n= 3). (B) In similar experiments, LDN-treated and controls cells were administered thrombin (1 unit/ml) or vehicle and TER was measured. At the nadir of TER changes, thrombin-induced barrier disruption was significantly increased in UCHL1-silenced cells (bar graph, *p < 0.05, n = 3).

Figure 3. Redistribution of VE-cadherin and β-catenin in UCHL1-silenced EC. (A) Immunofluorescence imaging of EC transfected with control siRNA (nsRNA) or siUCHL1 (100 nM, 3 d) demonstrate co-localization of VE-cadherin and β-catenin at the cell periphery in control cells (arrows). In contrast, UCHL1-silencing demonstrated reduced levels of VE-cadherin and β-catenin at the membrane with redistribution to the cytoplasm (representative images shown). **(B)** Notably, Western blotting of whole cell lysates confirmed significantly reduced total VE-cadherin levels in UCHL1-silenced EC (representative blot shown, *p < 0.05, n = 3).

Figure 4. Proteasomal degradation of VE-cadherin is increased in response to UCHL1 silencing. (A) EC transfected with siRNA (100 nM, 3 d) or non-specific RNA (control siRNA) were treated with chloroquine (20 μM, 2 h), a lysosomal inhibitor, prior to Western blotting. In response to UCHL1 silencing, levels of VE-cadherin Y658 phosphorylation were significantly increased while total VE-cadherin levels were significantly decreased (*p > 0.05 compared to respective controls transfected with non-

specific siRNA). However, chloroquine did not have a significant on either total or phospho-VE-cadherin. **(B)** In similar experiments, EC transfected with siRNA (100 nM, 3 d) or non-specific RNA (control siRNA) were treated with MG-132 (10 μM, 2 h), a proteasomal inhibitor, prior to Western blotting. In response to UCHL1 silencing, levels of VE-cadherin Y658 phosphorylation were significantly increased (*$p < 0.05$ compared to respective controls transfected with non-specific RNA). However, while silencing UCHL1 was associated with significantly decreased VE-cadherin phosphorylation at Y658, these effects were abrogated by pretreatment with MG132 (**$p < 0.05$). (n = 3/experimental condition) **(C)** Immunoprecipitation of VE-cadherin after UCHL1 silencing (100 nM, 3 d) followed by Western blotting for ubiquitin demonstrated an increased association of ubiquitin with VE cadherin (representative blots shown).

Figure 5. Claudin-5 expression is decreased in UCHL1-silenced EC. (A) Western blotting of UCHL1-silenced EC (100 nM, 3d) demonstrated decreased claudin-5 expression levels compared to controls transfected with control siRNA (* $p > 0.05$, n=3). **(B)** Immunofluorescence of UCHL1-silenced EC revealed decreased claudin-5 specifically localized at the cell membrane compared to controls. **(C)** Silencing of FoxO1 (siFoxO1, 100 nM, 3 d) abrogated the decreased expression of claudin-5 associated with UCHL1 knockdown (siUCHL1) (representative blots shown).

Figure 6. UCHL1 inhibition is associated with increased VILI: BAL fluid analysis.

C57Bl/6 mice were pretreated with the UCHL1 inhibitor LDN-57444 (LDN, 5 mg/kg, IP) or vehicle 24 h and again 1 h before VILI-challenge (V_T 30 ml/kg, 4 h). Bronchoalveolar lavage (BAL) was then collected for analysis of **(A)** total protein and **(B)** total cell counts as well as **(C)** differential cell counts. Compared to VILI-challenged control animals, LDN treatment was associated with significantly increased total protein and cell counts with significant increase specifically in PMNs (*$p < 0.05$, n = 3 animals/condition).

Figure 7. UCHL1 inhibition is associated with increased VILI: Lung Histology. C57Bl/6 mice were pretreated with the UCHL1 inhibitor LDN-57444 (LDN, 5 mg/kg, IP) or vehicle 24 h and again 1 h before VILI-challenge (V_T 30 ml/kg, 4 h). **(A)** Histology of lungs collected from select animals demonstrated interstitial edema and infiltration of inflammatory cells associated with VILI (bottom left panel) that was augmented by LDN treatment (bottom right panel; arrows indicate areas of edema and inflammatory cell infiltration; representative images shown).

Figure 8. Proposed schema of EC Barrier Regulation by UCHL1. UCHL1 promotes VE-cadherin expression levels via inhibition of its deubiquitination and subsequent proteasomeal degradation. In turn, VE-cadherin effects increased phosphorylation of FoxO1, a transcriptional repressor of claudin-5, leading to its translocation from the nucleus, as a result, increased claudin-5 expression. The combined effects of increased VE-cadherin and claudin-5 at the membrane augment EC barrier function. Conversely,

decreased UCHL1 expression is associated with increased proteasomal degradation of VE-cadherin which is preceded by its phosphorylation and internalization, events associated with adherens junction disassembly and decreased EC barrier function.

Figure 1.

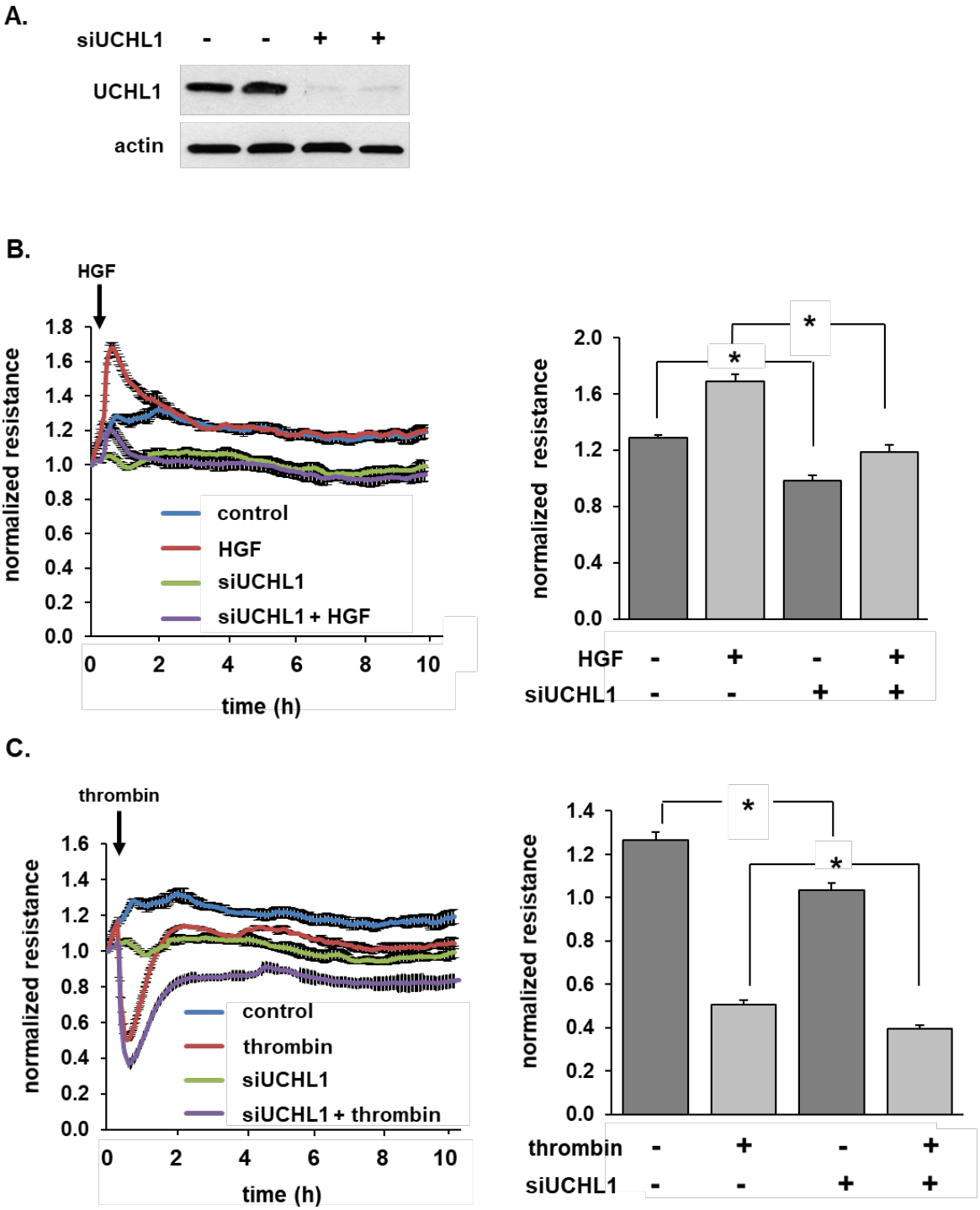
A.
siUCHL1 - - + +
UCHL1
actin
B.
HGF
normalized resistance
time (h)
control
HGF
siUCHL1
siUCHL1 + HGF
normalized resistance
HGF - + - +
siUCHL1 - - + +
C.
thrombin
normalized resistance
time (h)
control
thrombin
siUCHL1
siUCHL1 + thrombin
normalized resistance
thrombin - + - +
siUCHL1 - - + +

Figure 1.

D.

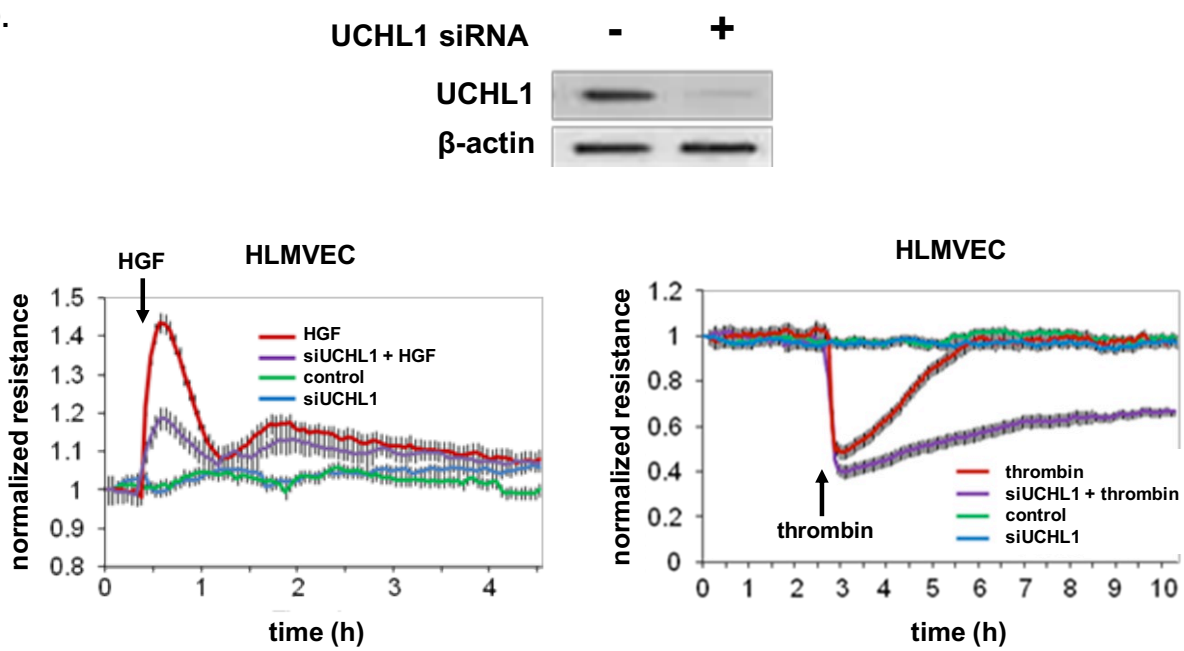
UCHL1 siRNA
-
+
UCHL1
β-actin
HGF
HLMVEC
normalized resistance
time (h)
HGF
siUCHL1 + HGF
control
siUCHL1
HLMVEC
normalized resistance
thrombin
thrombin
siUCHL1 + thrombin
control
siUCHL1
time (h)

Figure 3.

A.

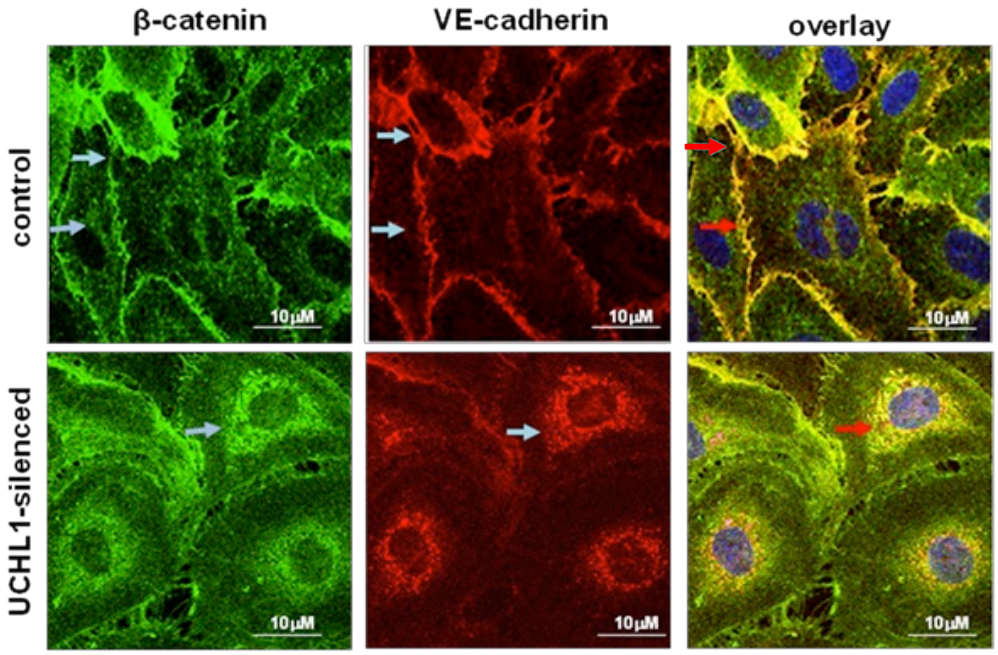
β-catenin
VE-cadherin
overlay
control
UCHL1-silenced
10μM

B.

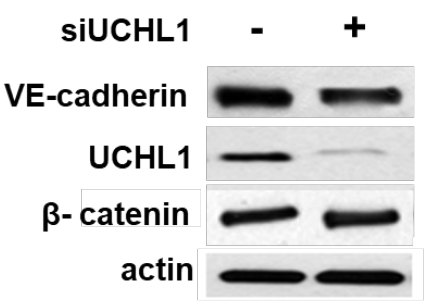
siUCHL1 - +
VE-cadherin
UCHL1
β- catenin
actin

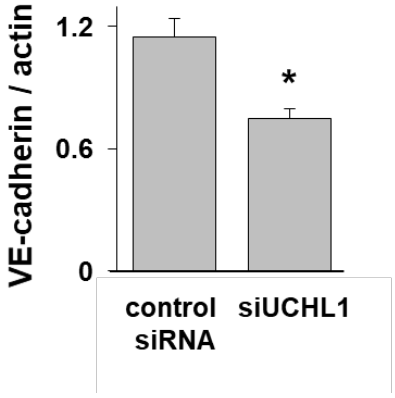
VE-cadherin / actin
1.2
0.6
0
*
control siRNA
siUCHL1

Figure 4.

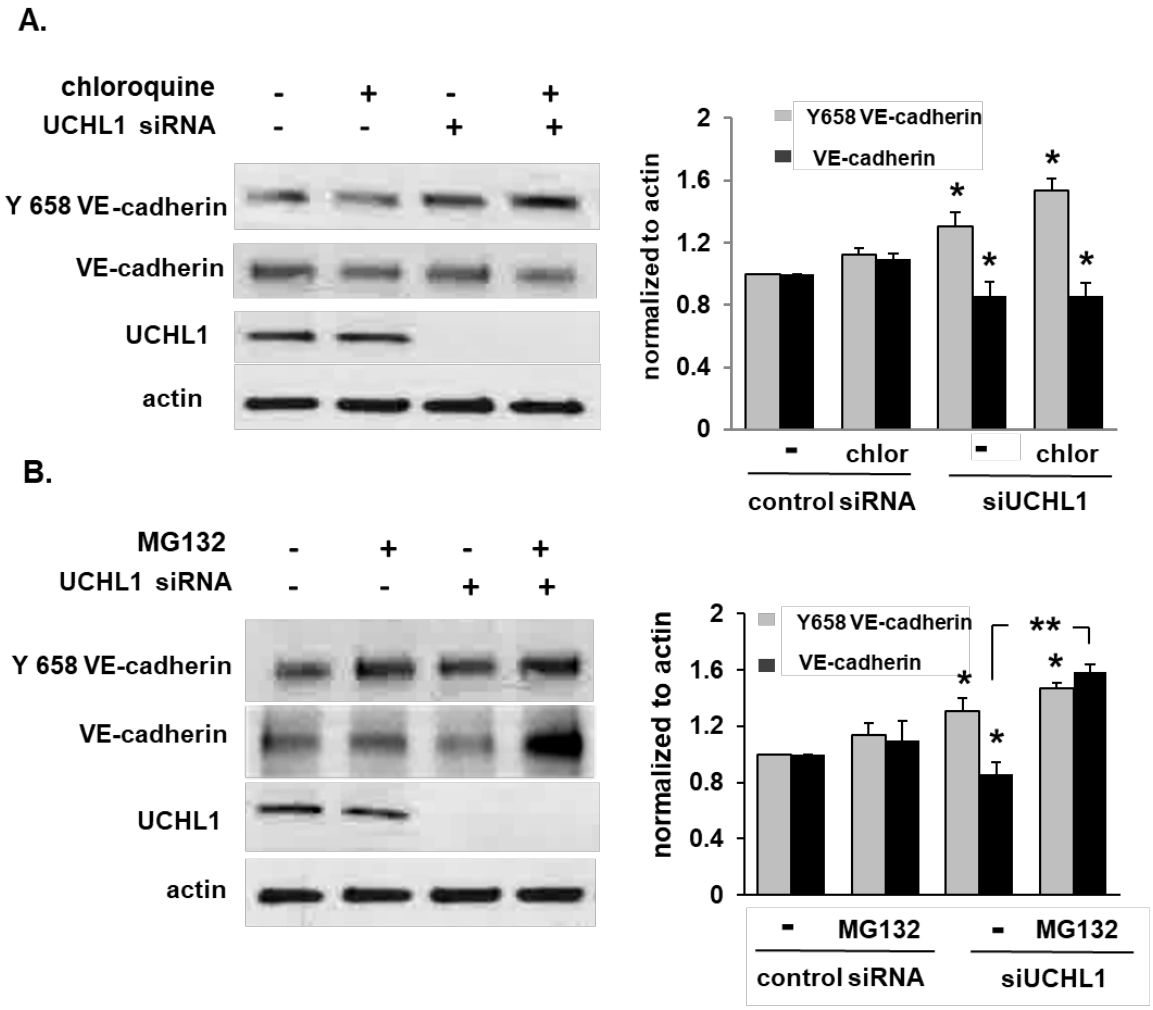
A.
chloroquine - + - +
UCHL1 siRNA - - + +
Y 658 VE-cadherin
VE-cadherin
UCHL1
actin
Y658 VE-cadherin
VE-cadherin
normalized to actin
2
1.6
1.2
0.8
0.4
0
- chlor - chlor
control siRNA
siUCHL1
B.
MG132 - + - +
UCHL1 siRNA - - + +
Y 658 VE-cadherin
VE-cadherin
UCHL1
actin
Y658 VE-cadherin
VE-cadherin
normalized to actin
- MG132 - MG132
control siRNA
siUCHL1

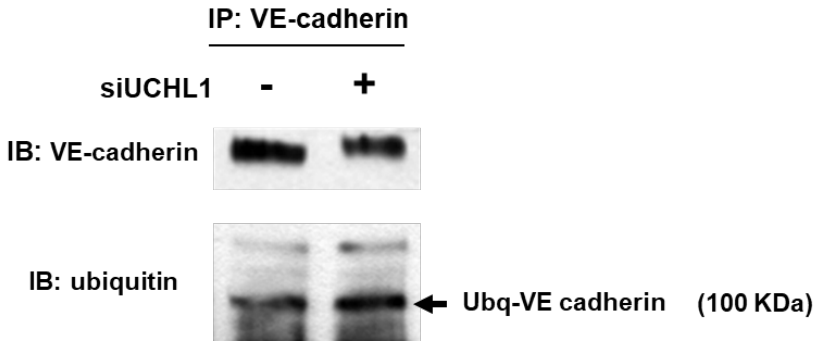
C.
IP: VE-cadherin
siUCHL1 - +
IB: VE-cadherin
IB: ubiquitin
Ubq-VE cadherin (100 KDa)

Figure 5.

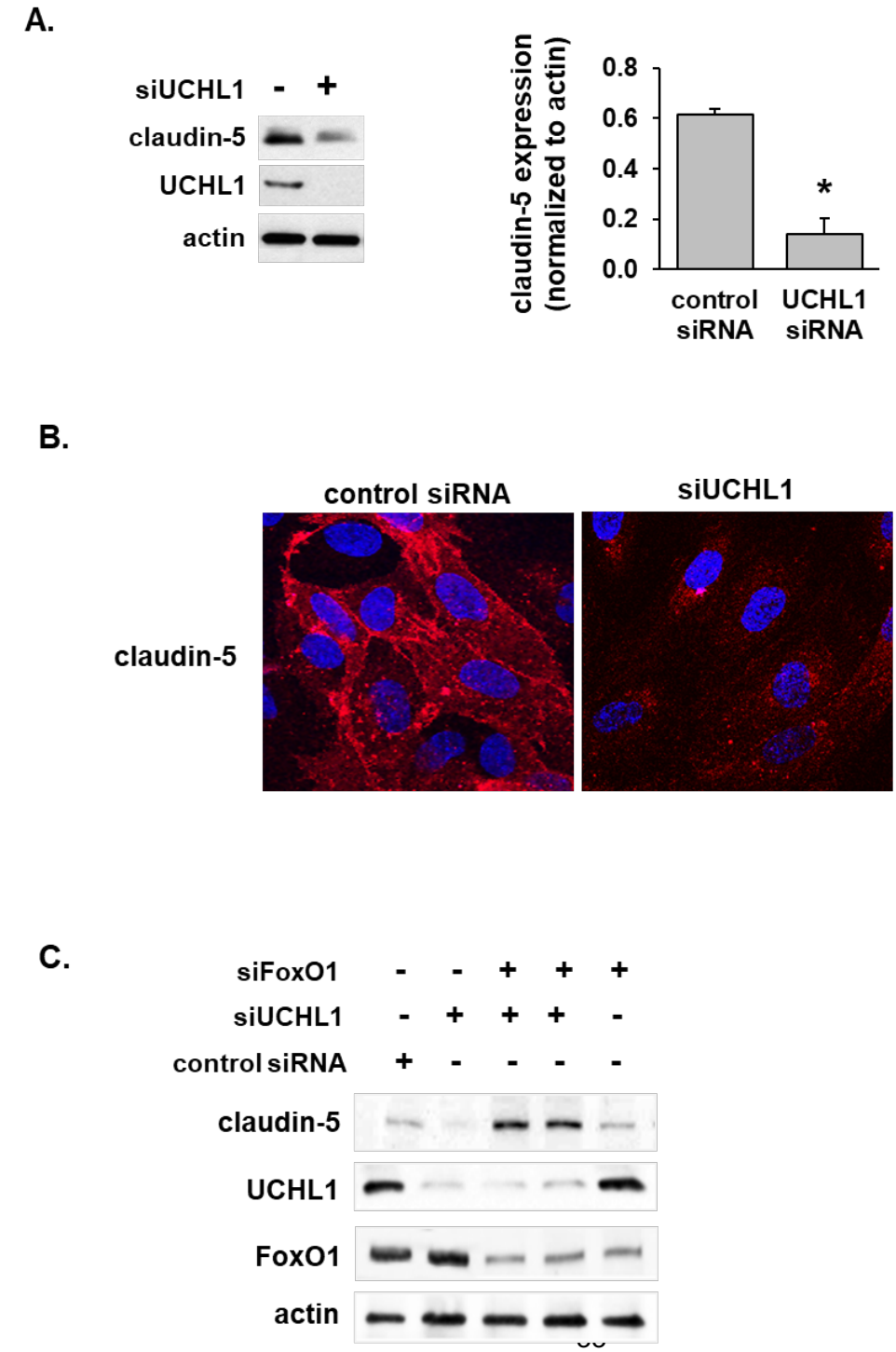
A.
siUCHL1 - +
claudin-5
UCHL1
actin
claudin-5 expression (normalized to actin)
0.8
0.6
0.4
0.2
0.0
*
control siRNA
UCHL1 siRNA
B.
control siRNA
siUCHL1
claudin-5
C.
siFoxO1 - - + + +
siUCHL1 - + + + -
control siRNA + - - - -
claudin-5
UCHL1
FoxO1
actin

Figure 6.

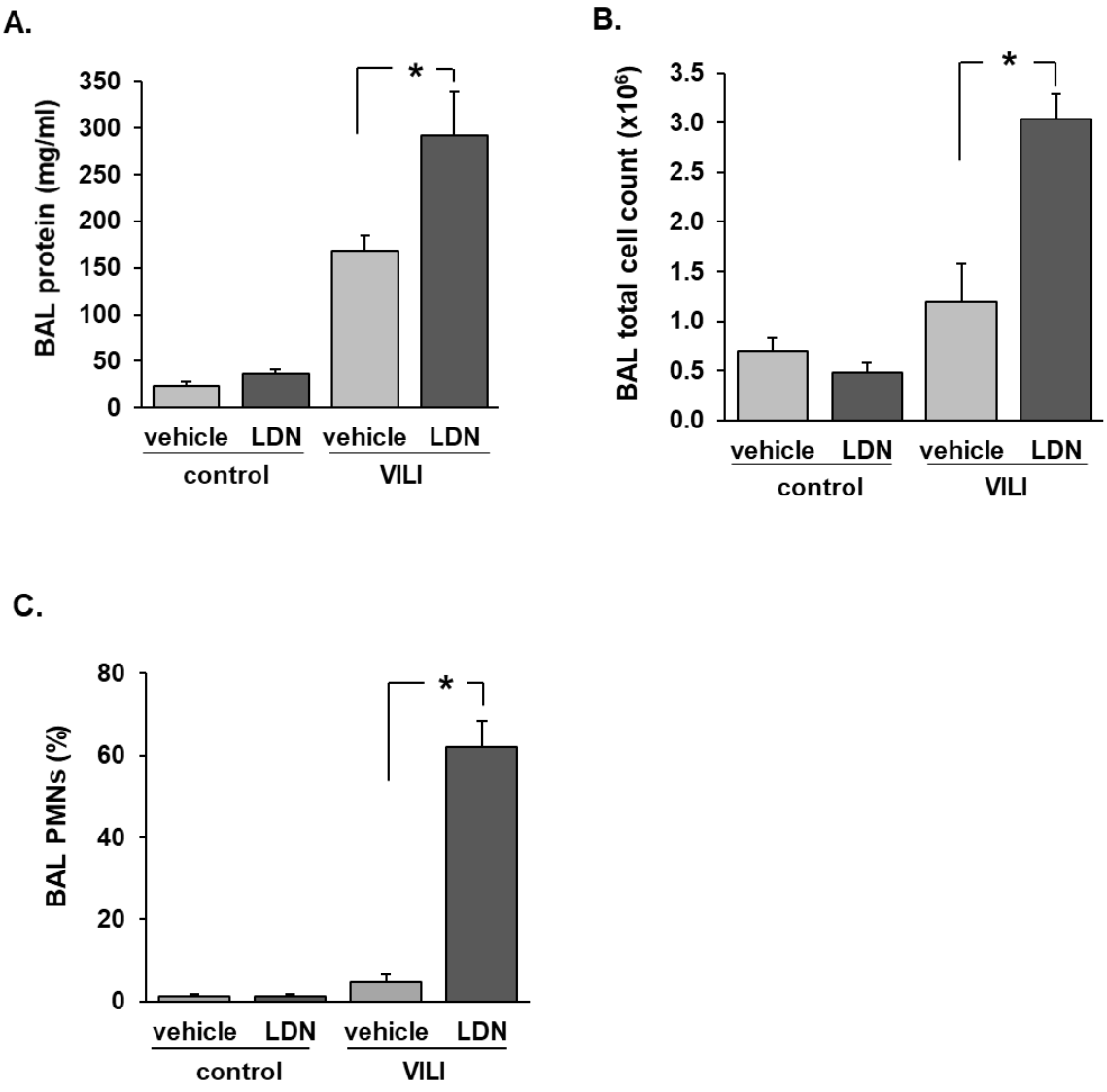
A.
BAL protein (mg/ml)
350
300
250
200
150
100
50
0
*
vehicle
LDN
vehicle
LDN
control
VILI
B.
BAL total cell count (x10^6)
3.5
3.0
2.5
2.0
1.5
1.0
0.5
0.0
*
vehicle
LDN
vehicle
LDN
control
VILI
C.
BAL PMNs (%)
80
60
40
20
0
*
vehicle
LDN
vehicle
LDN
control
VILI

Figure 7.

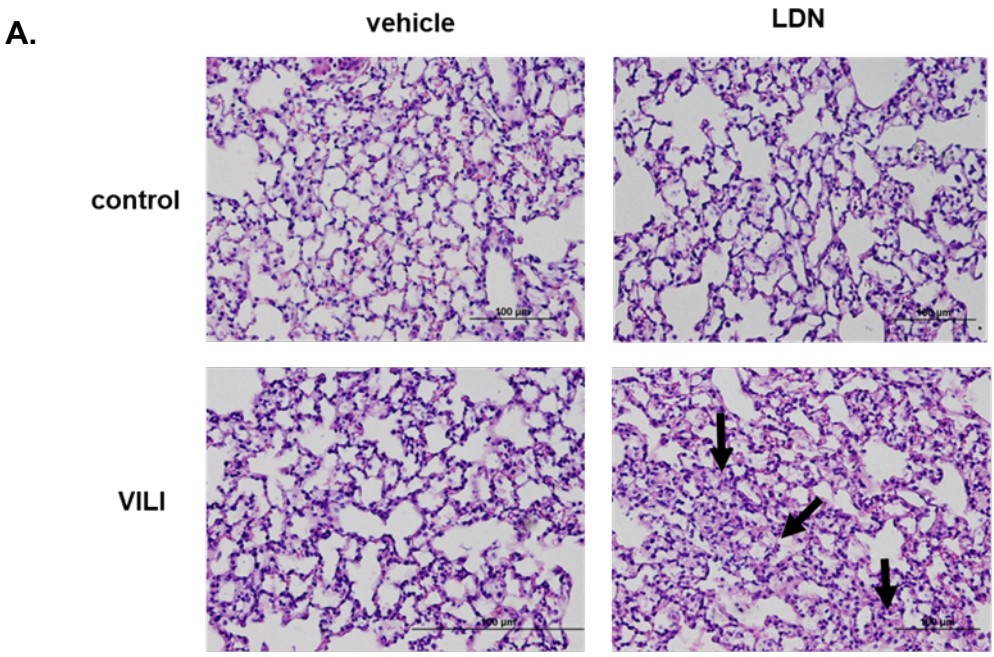

Figure 8.

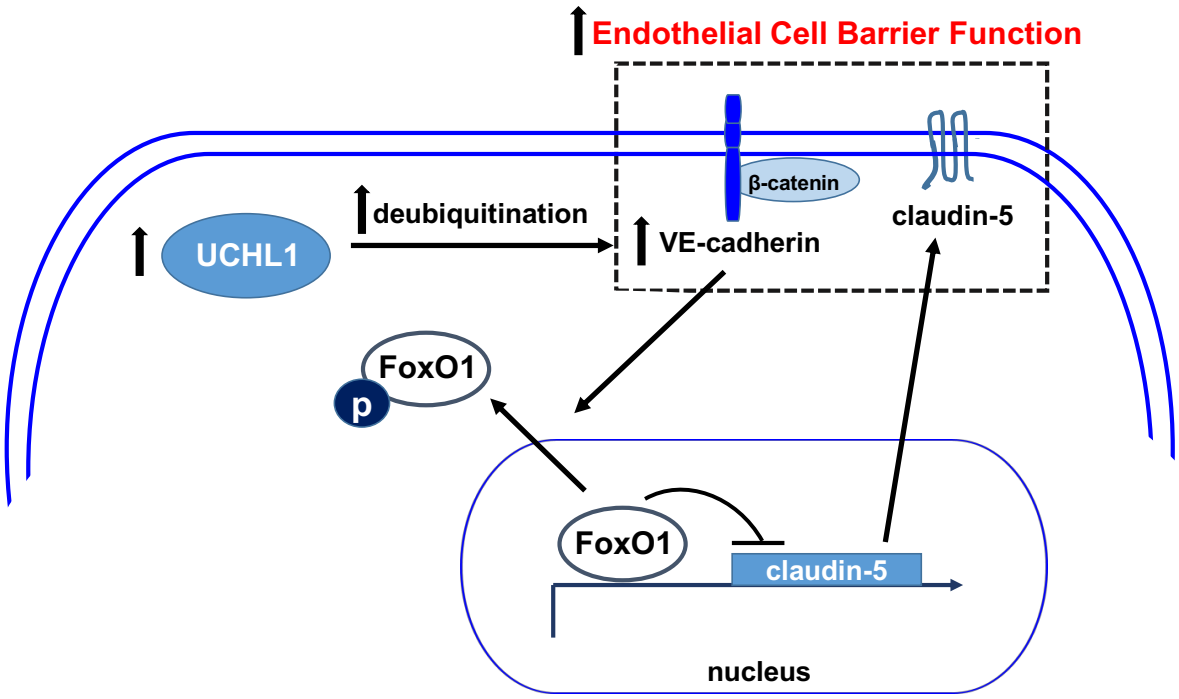
Endothelial Cell Barrier Function
β-catenin
claudin-5
deubiquitination
UCHL1
VE-cadherin
FoxO1
p
FoxO1
claudin-5
nucleus